Buckling and Nonlinear Response of Imperfect Three-Legged Truss Columns

Dov Elyada* and Charles D. Babcock†
California Institute of Technology, Pasadena, California

A closed-form theoretical investigation of the nonlinear structural behavior of idealized imperfect three-legged truss columns is presented. The columns examined have equilateral-triangular cross sections formed by three longerons held in place by equally spaced battens. The columns are simply supported and loaded by a pure axial compressive force. Local as well as global finite geometrical imperfections are admitted. Closed-form expressions are obtained for local and global buckling, postbuckling, imperfection sensitivities, nonlinear response, and limit loads. Local-global mode interaction is accounted for fully. Comparisons are made with numerical results and those in the literature.

Introduction

In recent years, truss columns have been proposed as building blocks of many large space structure concepts. These structural components, being themselves built up, posses local as well as global modes of buckling. It is known for a long time[1,2] that such structures may exhibit "mode interaction," i.e., whereas each mode considered separately is imperfection insensitive, their interaction produces a highly imperfection-sensitive structure. This is especially true if the corresponding buckling loads are close. Weight optimization, so crucial in space applications, tends to create exactly this circumstance.[3] There is no way, then, that either realistic load-carrying capacity estimates or valid structural optimization be done without taking account of imperfection sensitivities brought about by mode interaction. The purpose of this work is thus twofold: to present another example by means of which the phenomenon of modal interaction may be studied and to go a step further toward providing a realistic design tool for the class of structures under consideration.

We consider an *idealized* simply supported three-legged truss column (Fig. 1), loaded in pure axial compression. Here, "idealized" means that transverse shear is carried by an unspecified web of infinite rigidity that does not modify the longeron forces. The longerons ("legs") are assumed discontinuous, their segments (between battens) being pinned to each other as well as to the battens. Local (longeron segments) as well as global (column axis) geometrical imperfections are admitted, consisting of sine half-waves with half-wavelengths of a segment and the whole column, respectively. Sought is the complete nonlinear behavior of the general column and that of associated special cases.

The problem under study can be traced to the monograph by Thompson and Hunt,[2] where a globally perfect two-legged strut is analyzed for global buckling using a Shanley formula approach. A similar treatment is found in Crawford and Hedgepeth.[4] A continuous-longeron variant serves as an example in a work by Byskov.[5] Mikulas[6] deals with three-legged columns having only global imperfection. A step toward applicability was made by Crawford and Benton.[7] They introduced hypotheses that presumably enable the extension of Thompson and Hunt's method to the full problem. Such hypotheses are avoided in the present work, in which the approach is fundamental.

The present analysis is based on a column deflection differential equation derived in the first section. Exact solutions are then obtained for the globally and locally perfect special cases. For the general case, an equilibrium path relation is derived by means of a weighted residual method combined with an identification technique. This is then analyzed to reveal features such as local and global buckling, ultimate strength, and imperfection sensitivities. Comparisons are made with results in the literature as well as with those of direct numerical integration.

Deflection Differential Equation

First, a relation is derived between the shortening $\Delta\ell$ of an imperfect longeron segment and the axial compressive (local) load p acting on it. Let the segment length be ℓ, its bending and axial stiffnesses be EI and EA, respectively, and its initial (imperfection) shape be $\bar{\epsilon}\sin(\pi\xi/\ell)$. See Fig. 1. $\bar{\epsilon}$ will serve as a local imperfection parameter. Being by assumption pinned at both ends and provided its deflection is small, the segment shortens according to

$$\frac{\Delta\ell}{\ell}=\frac{\pi^2(\bar{\epsilon}/\ell)^2}{4}\left[\frac{1}{(1-p/p_e)^2}-1\right]+\frac{p}{EA} \tag{1}$$

where p_e is the segment Euler buckling load π^2EI/ℓ^2. From a global standpoint, Eq. (1) can be interpreted as a "stress-strain" relation. We now proceed to determine a corresponding (global) "strain-displacement" relation.

Since Crawford and Benton[7] have found that global imperfection is most detrimental to column strength when occurring in a plane bisecting the column cross section, we will limit our attention to deflections in the $(\bar{x},\bar{z})$ plane of Fig. 1. It seems plausible that this plane accomodates a preferred global buckling direction also in the globally perfect case. Also, if the column consists of a sufficiently large number of bays, it is justifiable to regard it as a one-dimensional continuum and its deflection in the $\bar{z}$ direction as a continuous, twice-differentiable function $\bar{w}(\bar{x})$. Its second derivative $\bar{w}''(\bar{x})$ can then be identified with the change in batten rotations across a bay divided by ℓ, an identification made possi-

Received Nov. 4, 1985; presented as Paper 86-0974 at the AIAA/ASME/ASCE/AHS 27th Structures, Structural Dynamics and Control Conference, San Antonio, TX, May 19-21, 1986.

*Graduate Student (presently, Senior Research Scientist and Head, Structures Section, Israel Armament Development Authority, Haifa, Israel). Member AIAA.

†Professor of Aeronautics and Applied Mechanics. Member AIAA.

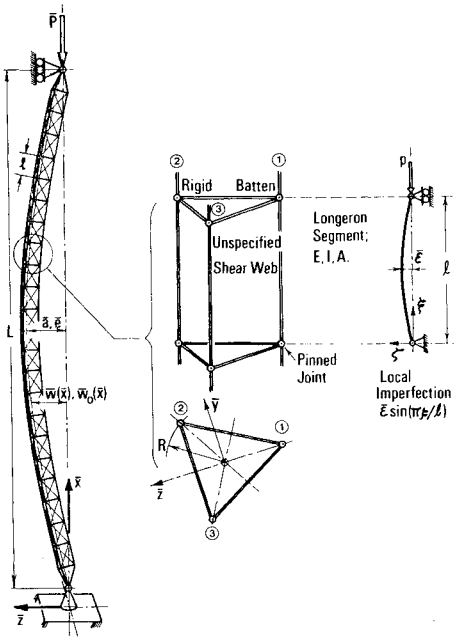

Fig. 1 Problem definition and notation.

Fig. 2 Global equilibrium.

ble by the assumed infinite shear rigidity. The sought strain-displacement relation then emerges in the form

$$(\Delta\ell/\ell)_1 - (\Delta\ell/\ell)_2 = -(3R/2)(\bar{w}'' - \bar{w}_0'') \tag{2}$$

where the subscripts 1 and 2 refer to the longerons designation in Fig. 1, R is shown in the same figure, and $\bar{w}_0(x)$ is the global imperfection deflection.

There remains to determine equilibrium relations between the internal longeron forces $p_1(\bar{x})$, $p_2(\bar{x})$, $p_3(\bar{x})$ and the external load $\bar{P}$. This is done with the aid of Fig. 2, yielding

$$p_1 = \frac{\bar{P}}{3}\left(1+\frac{2\bar{w}}{R}\right); \quad p_2 = p_3 = \frac{\bar{P}}{3}\left(1-\frac{\bar{w}}{R}\right) \tag{3}$$

It is convenient to work with the following nondimensional quantities:

$$P \equiv \bar{P}/3p_e \tag{4}$$

$$w \equiv \bar{w}/R \tag{5}$$

$$\epsilon \equiv \bar{\epsilon}/\sqrt{2I/A} = \bar{\epsilon}/\sqrt{2}\rho \tag{6}$$

$$x \equiv \pi\bar{x}/L \tag{7}$$

$$P_E \equiv \frac{1}{2}\frac{(\ell/\rho)^2}{(L/R)^2} \tag{8}$$

where ρ is the longeron bending-related cross-sectional radius of gyration $\sqrt{I/A}$ and L (Fig. 1) the column length. P_E is nothing but the nominal (perfect column) global Euler buckling load normalized by $3p_e$. Eliminating p and $(\Delta\ell/\ell)$ in Eqs. (1-3) in favor of $\bar{w}$ and $\bar{w}''$ and normalizing according to Eqs. (4-8), we obtain one form of the desired differential equation,

$$P_E(w'' - w_0'') + Pw + \frac{\epsilon^2}{6(1-P)^2}\left\{\frac{1}{[1-2wP/(1-P)]^2} - \frac{1}{[1+wP/(1-P)]^2}\right\} = 0 \tag{9}$$

It is advantageous to represent the deflection by still another function, $\varphi(x)$, the absolute maximum of which we denote by α,

$$\varphi(x) \equiv \frac{2P}{1-P}\,w(x), \qquad \alpha = \frac{2P}{1-P}\,a \tag{10}$$

where a is the absolute maximum of $w(x)$. In terms of φ, the deflection differential equation becomes

$$P_E(\varphi'' - \varphi_0'') + P\varphi + \frac{\epsilon^2 P}{3(1-P)^3}\left[\frac{1}{(1-\varphi)^2} - \frac{1}{(1+\varphi/2)^2}\right] = 0 \tag{11}$$

Solutions of Eq. (11) are required to satisfy the simply supported boundary conditions $\varphi(0) = \varphi(\pi) = 0$, and these restrict the possible (a,P) pairs along lines in the a-P plane we call "equilibrium paths."

The Locally Perfect Case, Local Buckling

Equation (11) is singular at points where $\varphi = 1$. (The case $\varphi = -2$ is of no relevance here.) This singularity can be traced to $p_1 = p_e$ and is therefore referred to as "local buckling." It first comes into play when $\alpha = 1$, since $\alpha \equiv \max[\varphi(x)]$. By Eq. (10), $\alpha = 1$ describes a locus in the a-P plane (Fig. 3) we call the "local buckling line" (LBL).

$$P = 1/(1+2a) \equiv P_{\mathrm{LB}} \tag{12}$$

Consider now the locally perfect limit of Eq. (11). First multiply Eq. (11) by $(1-\varphi)^2$ and then let $\epsilon^2 P/(1-P)^3 \to 0$,

$$(1-\varphi)^2[P_E(\varphi'' - \varphi_0'') + P\varphi] = 0 \tag{13}$$

If $\alpha < 1$, the first factor in Eq. (13) never comes into play and, for $w_0 = e\sin x$, the classical Euler solution is obtained,

$$w = a\sin x; \qquad a = \frac{e}{1 - P/P_E} \tag{14a,b}$$

where e is the normalized global imperfection amplitude. We call the function in Eq. (14a) the "global mode" and the associated equilibrium path, Eq. (14b), the "global line." On the other hand, if $\alpha = 1$, there exists a point $x = x_{\ell b}$ where $\varphi = 1$. It is then possible to satisfy Eq. (13) at that point with any, even infinite, φ'', provided its singularity is weaker than that of $(1-\varphi)^{-2}$. Moreover, the arbitrariness of φ'' allows satisfaction of the boundary conditions as well. Such a solution ($\varphi_0 \equiv 0$ is taken for simplicity) is given by

$$\varphi(x) = \frac{\sin\sqrt{(P/P_E)}\,x}{\sin\sqrt{(P/P_E)}\,x_{\ell b}}, \qquad 0 \le x \le x_{\ell b}$$

$$= \frac{\sin\sqrt{(P/P_E)}\,(\pi - x)}{\sin\sqrt{(P/P_E)}\,(\pi - x_{\ell b})}, \qquad x_{\ell b} \le x \le \pi \tag{15}$$

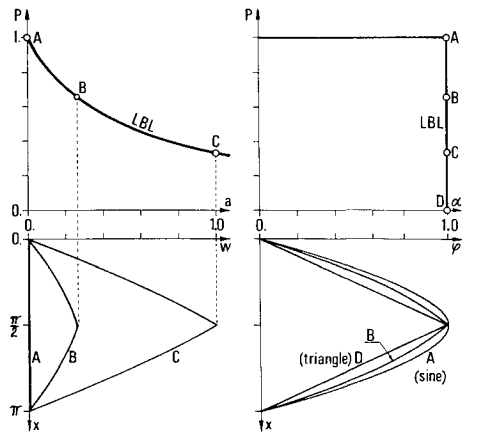

Fig. 3 Local buckling line and corresponding deflection shapes for $P_E=1$ and $x_{lb}=\pi/2$.

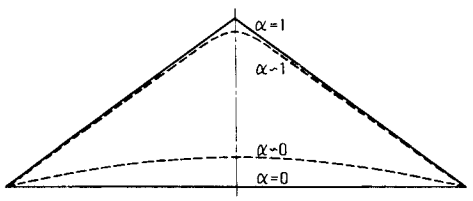

Fig. 4 Postbuckling deflection shape as function of α (qualitative).

We call Eq. (15) the "local mode" (Fig. 3). Its associated equilibrium path is clearly the LBL, Eq. (12). The δ-function singularity of φ'' at x_{lb} signifies the collapsing of the bay there. x_{lb} itself is indeterminate, except by history. Since the limit responsible for Eq. (13) is $\epsilon^2 P/(1-P)^3 \to 0$, we see that the LBL is an equilibrium path for all $a>0$ if $\epsilon=0$ and for all ϵ if $a\to\infty$.‡ Note that, by Eq. (13), as $a\to\infty$ (i.e., $P\to 0$), the local mode becomes triangular.

The Globally Perfect Case, Global Buckling and Postbuckling

By "global buckling," we refer to the bifurcation of a globally perfect column from a globally undeflected (prebuckled) state into a deflected one. Thereafter, the column is said to be postbuckled. Only the lowest P bifurcation is treated here and, accordingly, a single half-wave solution is assumed.

Let $\varphi_0=0$, multiply Eq. (11) by $2\varphi'/P_E$ and integrate

$$\varphi'^2+\frac{P}{P_E}\varphi^2+\frac{2}{3}\frac{P/P_E}{(1-P)^3}\epsilon^2\left(\frac{1}{1-\varphi}+\frac{2}{1+\varphi/2}\right)=\text{const} \tag{16}$$

Provided $P<P_{\text{LB}}$, a single half-wave mode satisfies $(\varphi'=0) \Leftrightarrow (\varphi=\alpha)$. Use this to express the constant of integration in terms of α,

$$\varphi'=\pm\left\{\frac{P}{P_E}(\alpha^2-\varphi^2)+\frac{P}{P_E}\frac{\epsilon}{(1-P)^3}\left[\frac{\alpha^2}{(1-\alpha)(1+\alpha/2)}-\frac{\varphi^2}{(1-\varphi)(1+\varphi/2)}\right]\right\}^{1/2} \tag{17}$$

‡That these are also necessary conditions can be seen from solving asymptotically in the neighborhood of x_{lb} for $\alpha=1$, $\epsilon^2P/(1-P)^3>0$ to get $\phi\sim 1+(3\epsilon^2P/2P_E)^{1/3}(1-P)^{-1}(x-x_{lb})^{2/3}\geq 1$, $x\to x_{lb}$.

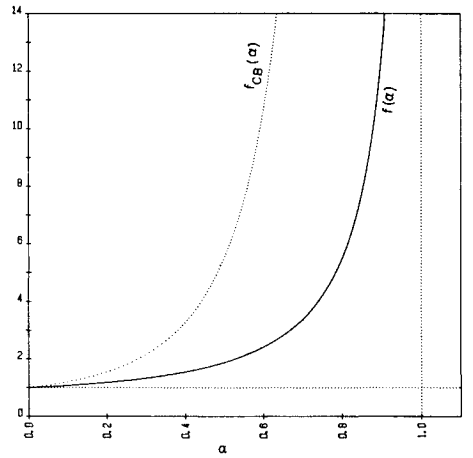

Fig. 5 Functions $f(\alpha)$ [Eq. (25)] and $f_{\text{CB}}(\alpha)$ [Eq. (35)].

The ascending leg of the solution is now obtained by integrating the positive branch of Eq. (17) and changing variable $\varphi=\alpha t$,

$$x(\varphi)=\sqrt{\frac{P_E}{P}}\int_0^{\varphi/\alpha}\frac{dt}{\sqrt{1-t^2}}\times\left[1+\frac{\epsilon^2}{(1-P)^3}\frac{1-(\alpha t/2)/(1+t)}{(1-\alpha)(1+\alpha/2)(1-\alpha t)(1+\alpha t/2)}\right]^{-1/2},\qquad 0\leq\varphi\leq\alpha \tag{18}$$

This already satisfies the $x=0$ boundary condition. On account of the (obvious) evenness of $\varphi(x)$ about the midspan, Eq. (18) suffices as a solution provided the $\varphi(\pi)=0$ condition is replaced by $\varphi(\pi/2)=\alpha$. When the latter is applied to Eq. (18), it gives rise to the postbuckling α-P equilibrium path,

$$\frac{\pi}{2}=\sqrt{\frac{P_E}{P}}\int_0^{1}\frac{dt}{\sqrt{1-t^2}}\times\left[1+\frac{\epsilon^2}{(1-P)^3}\frac{1-(\alpha t/2)/(1+t)}{(1-\alpha)(1+\alpha/2)(1-\alpha t)(1+\alpha t/2)}\right]^{-1/2} \tag{19}$$

To gain insight into the column behavior, it is useful to examine the asymptotic behavior of the results, Eqs. (18) and (19), at both ends of the α range. For $\alpha\to 0$ we obtain

$$x(\varphi)\sim\arcsin\frac{\varphi}{\alpha}+\frac{\alpha}{2}\left(1-\frac{P}{P_E}\right)\left[\left(\frac{2}{\pi}\arcsin\frac{\varphi}{\alpha}-1\right)+\left(1+\frac{\varphi}{2\alpha}\right)\sqrt{\frac{1-\varphi/\alpha}{1+\varphi/\alpha}}\right] \tag{20}$$

$$(P_E-P)(1-P)^3-\epsilon^2P\left(1+\frac{2}{\pi}\alpha\right)\sim 0 \tag{21}$$

The first of these has an inversion of the form $\varphi=\alpha\sin x+\mathcal{O}(\alpha^2)$, meaning that as $\alpha\to 0$ the deflection becomes that of an ordinary Euler column. The $\mathcal{O}(\alpha^2)$ term can be shown to make the deflection more "pointed" at the midspan as α increases. Equation (21) describes the initial postbuckling equilibrium path.

We now let $\alpha \to 1$ close enough that $\epsilon^2/(1-\alpha) \gg 1$. From Eq. (17) we obtain

$$\varphi' = \sqrt{\frac{2(P/P_E)}{3(1-P)^3} \cdot \frac{\epsilon^2}{1-\alpha}} = \text{const}, \qquad \varphi < \alpha$$

$$\varphi' = 0, \qquad \varphi = \alpha \tag{22}$$

Applying $\varphi(\pi/2) = \alpha$ to these, the asymptotic as $\alpha \to 1$ equilibrium path is found,

$$P_E(1-P)^3 - \epsilon^2 P \frac{\pi^2/6}{1-\alpha} \sim 0 \tag{23}$$

In agreement with the results obtained in the previous section, the large-deflection equilibrium path is seen to be asymptotic to the LBL; the corresponding deflection shape tending to the triangular. Figure 4 shows the deflection shape as it varies along a postbuckling path.

Approximate General Equilibrium Path

If both imperfection modes are present, an exact, closed-form solution of Eq. (11) is no longer feasible. An approximate equilibrium path relation can nevertheless be obtained as follows. Let $\varphi = \psi(\alpha, x)$ be an *assumed* deflection shape satisfying the boundary conditions. Due to its explicit independence of P_E, ϵ, and e, ψ cannot satisfy Eq. (11) except in some average sense. We can impose this by employing a one-term weighted residual method such as Galerkin's. (See, e.g., Brebbia,[8] Chap. 2.) This leads to

$$[P_E - g(\alpha)P](1-P)^3 - 2eP_E P(1-P)^2 h(\alpha) - \epsilon^2 P f(\alpha) = 0 \tag{24}$$

where $f(\alpha)$, $g(\alpha)$, and $h(\alpha)$, yet to be determined, stem from certain spanwise integrals involving ψ, ψ'', and φ_0''. Some confidence in the $\varphi = \psi(\alpha, x)$ assumption can be gained from the fact that Eqs. (21) and (23) do conform with Eq. (24). Since a good ψ is hard to guess, we will not attempt to calculate f, g, and h from their definitions; instead, we will *identify* them, drawing upon the limiting cases, Eqs. (14b) and (19).

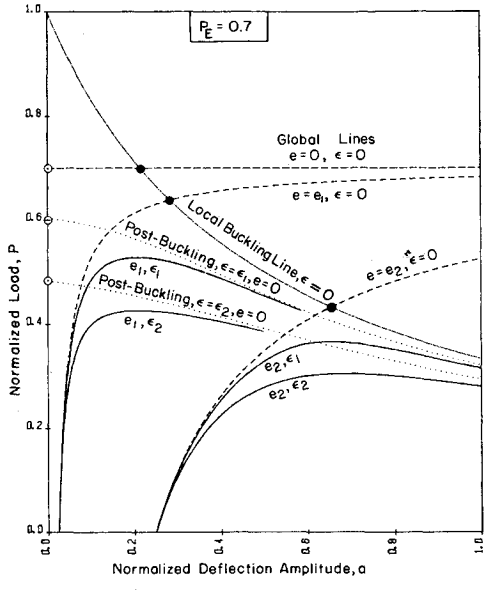

Fig. 6 Typical equilibrium paths of the doubly imperfect column for $P_E < 1$ ($\epsilon_1 = 0.10$, $\epsilon_2 = 0.25$, $e_1 = 0.025$, $e_2 = 0.25$); ○ global bifurcation, ● local bifurcation.

For $e = 0$, rewrite Eq. (24) in the form

$$\sqrt{\frac{P}{P_E}} \left\{ \frac{\pi}{2} \left[g(\alpha) + \frac{\epsilon^2}{(1-P)^3} f(\alpha) \right]^{-1/2} \right\} = \frac{\pi}{2}$$

and consider it *identical* to Eq. (19). Taking $\epsilon^2/(1-P)^3 \to 0$, we get $g(\alpha) = 1$. Taking it to infinity, we find

$$f(\alpha) = \frac{\pi^2/4}{(1-\alpha)(1+\alpha/2)} \left\{ \int_0^1 \sqrt{\frac{(1-\alpha t)(1+\alpha t/2)}{(1-t)[1+(1-\alpha/2)t]}}\, dt \right\}^{-2} \tag{25}$$

It is worthwhile to note that $f(\alpha)$ thus identified satisfies both limiting cases implied by Eqs. (21) and (23), namely,

$$f(\alpha) \sim 1 + (2/\pi)\alpha, \quad \alpha \to 0 \tag{26a}$$

$$f(\alpha) \sim (\pi^2/6)/(1-\alpha), \quad \alpha \to 1 \tag{26b}$$

Figure 5 depicts $f(\alpha)$. On the other hand, $g(\alpha) = 1$ agrees with Eq. (21), but, seemingly, not with Eq. (23). One has to note, however, that by Eq. (22) and the boundedness of φ', $P = \mathcal{O}(1-\alpha)$ as $\alpha \to 1$; hence, the disagreement is of no consequence.

In a similar way, we now let $\epsilon = 0$ in Eq. (24) and identify it with the corresponding special case [Eq. (14b)]. Again we find $g(\alpha) = 1$, and also, using Eq. (10), $h(\alpha) = 1/\alpha$. Thus, the

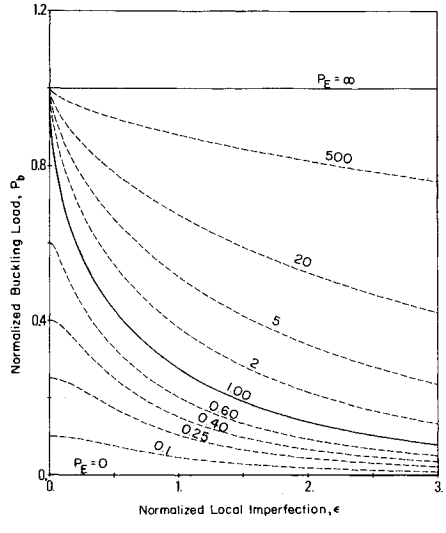

a) Dependence on ϵ and P_E.

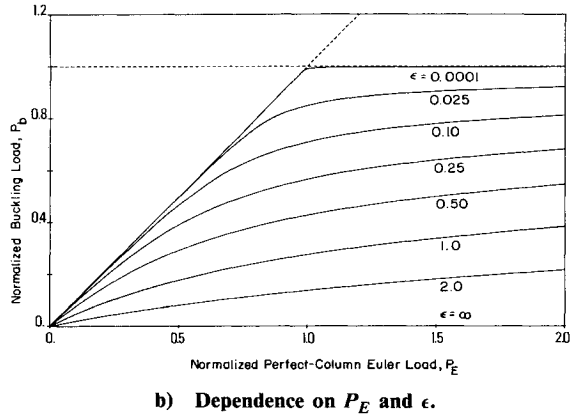

b) Dependence on P_E and ϵ.

Fig. 7 Global buckling load.

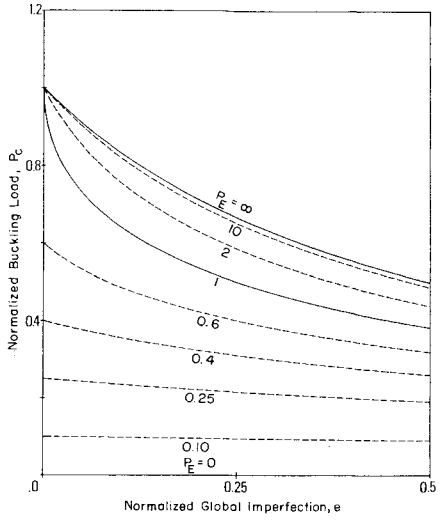

a) Dependence on e and P_E.

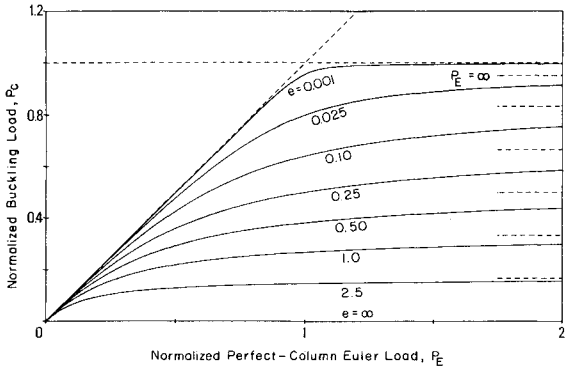

b) Dependence on P_E and e.

Fig. 8 Local buckling load.

approximate general equilibrium path relation is, finally

$$(P_E - P)(1-P)^3 - 2eP_E P(1-P)^2(1/\alpha) - \epsilon^2 P f(\alpha) = 0 \quad (27)$$

where $f(\alpha)$ is given by Eq. (25).

Behavior in the a-P Plane

We now investigate the load-deflection behavior of the general column and that of special cases derived from it. The complete information is contained in Eq. (27). Consider first the perfect-column case $e=\epsilon=0$. Since Eq. (27) has simple poles at $\alpha=0$, $\alpha=1$, it reduces to $\alpha(1-\alpha)(P_E-P)(1-P)^3 = 0$, or

$$a(P_E - P)(P_{LB} - P)(1-P) = 0 \quad (28)$$

where P_{LB} is defined in Eq. (12). Four distinct equilibrium paths are seen to exist: $a=0$, the prebuckling path; $P=P_E$, the Euler postbuckling path; the LBL, in agreement with the discussion following Eq. (15); and $P=1$, which is above the LBL for all $a>0$. The column follows the path of lowest P and therefore bifurcations occur. Two types of bifurcation are identified: "global," from $a=0$ to $P=P_E$ and "local," from $P=P_E$ to $P=P_{LB}$. This behavior is depicted in Fig. 6 for $P_E<1$. If P_E is increased, the two bifurcation points approach each other and coincide for $P_E=1$. For $P_E>1$ the global point is deactivated.

If only $e=0$, Eq. (27) reduces to an approximation of Eq. (19), the already discussed postbuckling equilibrium path (Fig. 6). This path departs from the $a=0$ path at $P=P_b$, the "global buckling load," an equation for which is obtained

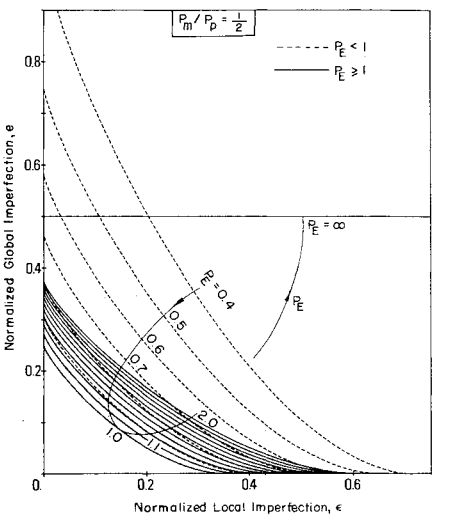

Fig. 9 Total finite-imperfection sensitivity chart.

by letting $\alpha=0$ in Eq. (21),

$$(P_E - P_b)(1-P_b)^3 - \epsilon^2 P_b = 0 \quad (29)$$

which agrees with the result of Thompson and Hunt (Ref. 2, p. 280). Shown in Fig. 7 is the variation of P_b with varying ϵ and P_E. The extreme sensitivity of P_b to ϵ, especially when $P_E=1$, is striking indeed. Of special interest are the asymptotic (as $\epsilon \to 0$) imperfection sensitivities of P_b. From Eq. (29),

$$P_b \sim P_E\left[1 - \frac{\epsilon^2}{(1-P_E)^3}\right], \qquad 0 < (1-P_E) = \mathcal{O}(1) \quad (30a)$$

$$P_b \sim 1 - \epsilon^{1/2}, \qquad |1-P_E| = o(\epsilon) \quad (30b)$$

$$P_b \sim 1 - (P_E - 1)^{-1/3}\epsilon^{2/3}, \qquad 0 < (P_E - 1) = \mathcal{O}(1) \quad (30c)$$

Note the increased sensitivity as $P_E \to 1$ from either side.

If only $\epsilon=0$, Eq. (27) reduces to

$$(1-P)^3(P_{LB} - P)[P_E(1 - e/a) - P] = 0 \quad (31)$$

Thus, active are the LBL and the global line [Eq. (14b)]; see Fig. 6. The bifurcation between them is of the local type, its P value given by

$$P_C = \frac{1}{2}\left[1 + P_E(1+2e) - |1-P_E|\sqrt{1 + 4eP_E\frac{1+(1+e)P_E}{(1-P_E)^2}}\right] \quad (32)$$

This was obtained by Mikulas[6] for $P_E=1$. P_C is shown graphically in Fig. 8 for varying e and P_E. The asymptotic (as $e \to 0$) imperfection sensitivities of P_C are found from Eq. (32) to be

$$P_C \sim P_E\left(1 - \frac{2eP_E}{1-P_E}\right), \qquad 0 < \frac{1-P_E}{P_E} = \mathcal{O}(1) \quad (33a)$$

$$P_C \sim 1 - \sqrt{2e}, \qquad |1-P_E| = o(\epsilon) \quad (33b)$$

$$P_C \sim 1 - \frac{2eP_E}{P_E - 1}, \qquad 0 < \frac{P_E - 1}{P_E} = \mathcal{O}(1) \quad (33c)$$

Again we see the increased sensitivity for $P_E=1$.

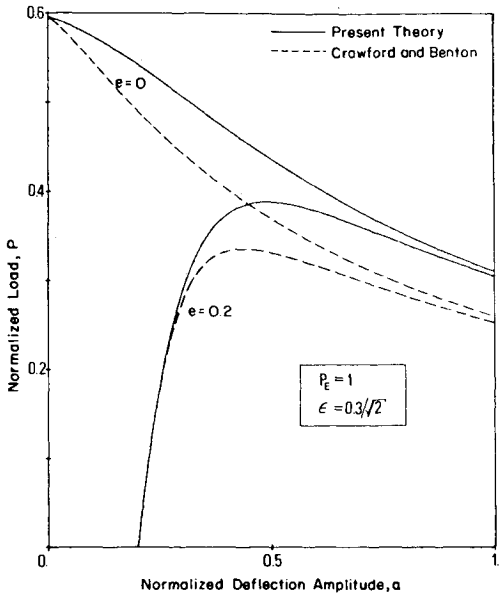

Fig. 10 Comparison of results with Crawford and Benton.[7]

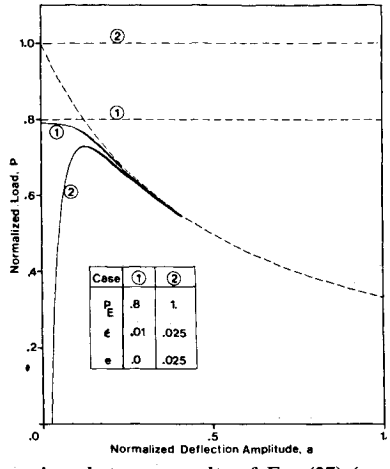

Fig. 11 Comparison between results of Eq. (27) (upper lines) and those of a 40 bay column finite-difference integration (lower lines).

When neither ϵ nor e vanish, we see (Fig. 6) that the path, representing the general nonlinear response of the column, is bounded from above by both the corresponding global line and postbuckling path. Thus, it has a maximum—the ultimate load-carrying capacity P_m—given implicitly by

$$e=\frac{(1-P_m)(P_E-P_m)}{2P_EP_m}\,\frac{\alpha^2 f'(\alpha)}{[\alpha f(\alpha)]'} \tag{34a}$$

$$\epsilon^2=\frac{(P_E/P_m-1)(1-P_m)^3}{[\alpha f(\alpha)]'} \tag{34b}$$

Figure 9 is a presentation based on Eqs. (34) of the finite (as opposed to asymptotic) total imperfection sensitivity. It gives, for different values of P_E, the combination of ϵ and e required to knock down the column strength to one-half its nominal value, $P_p \equiv \min(1,P_E)$. For $P_E=1$, this knockdown is seen to require the least amount of imperfection.

Comparisons with Ref. 7 and with Numerical Integration

In their paper, Crawford and Benton[7] extended the tangent modulus-Shanley formula approach of Thompson and Hunt[2] to cases including global bending. In doing so, they had to assume a spanwise-uniform tangent modulus, inconsistent with the spanwise-nonuniform internal forces. It can be shown that Eqs. (21) and (22) of Ref. 7 are equivalent, in our notation, to Eq. (27) here, with $f(\alpha)$ replaced by

$$f_{CB}(\alpha)\equiv\frac{2/3}{(1-\alpha)^3}+\frac{1/3}{(1-\alpha/2)^3} \tag{35}$$

shown for comparison in Fig. 5. This function is markedly different from our $f(\alpha)$ and, as can be seen from Fig. 10, so are the equilibrium paths it generates. (The paths $e=0.2$ in Fig. 10 correspond to the one given in Fig. 4 of Ref. 7.) It should be pointed out, however, that column strength thus calculated is, in general, conservative.

Comparison was also made with results of the direct numerical integration of a finite-difference version of Eq. (9), in which the bay was the basic interval and $\ell w''$ and w interpreted as the differential rotation and mean deflection of its deliminting battens. Satisfaction of the boundary conditions was achieved using shooting technique combined with Newton's method. The results (Fig. 11) show only slight deviation from those of Eq. (27), deviations that should be attributed to the assumption $\varphi=\psi(\alpha,x)$ and to Eq. (9) being a continuum approximation to its exact finite-difference counterpart.

Conclusions

The behavior of the subject column has been revealed by analysis based on the deflection differential equation (11). Apart from exact solutions for some special cases, the key result is Eq. (27), which describes the complete load-deflection nonlinear response. Features such as global buckling load [Eq. (29)], local buckling load [Eq. (32)], their respective asymptotic imperfection sensitivities [Eqs. (30) and (33)], and the limit load [Eqs. (34)] have been derived from it. The method devised for obtaining Eq. (27)—its success numerically proved—should be noted as potentially useful in many similar situations. The present theory has been shown to yield a much better approximation than previously available.

To what extent can idealized column results be applied to real columns? Recent work[9] undertaken to answer this question indicates that, as long as the column is slender, consists of a large number of bays, and has a properly sized shear web, the errors of idealization, although unconservative, are fairly small. Smaller still and conservative is the error committed in applying the present theory to continuous-longeron columns. Proofs of these results will be published in the future.

Acknowledgment

This work was supported in part by the California Institute of Technology President's Fund, Grant PF 218. This support is gratefully acknowledged.

References

[1]Van der Neut, A., "The Interaction of Local Buckling and Column Failure of Thin-Walled Compression Members," *Proceedings of the 12th International Congress on Applied Mechanics*, Springer-Verlag, New York, 1969, pp. 389-399.

[2]Thompson, J. M. T. and Hunt, G. W., *A General Theory of Elastic Stability*, Wiley, New York, 1973.

[3]Thompson, J. M. T. and Lewis, G. M., "On the Optimum Design of Thin-Walled Compression Members," *Journal of the Mechanics and Physics of Solids*, Vol. 20, May 1972, pp. 101-109.

[4]Crawford, R. F. and Hedgepeth, J. M., "Effects of Initial Waviness on the Strength and Design of Built-Up Structures," *AIAA Journal*, Vol. 13, May 1975, pp. 672-675.

[5]Byskov, E., "Applicability of an Asymptotic Expansion for Elastic Buckling Problems with Mode Interaction," *AIAA Journal*, Vol. 17, June 1979, pp. 630-633.

[6]Mikulas, M. M., "Structural Efficiency of Long, Lightly Loaded Truss and Isogrid Columns for Space Applications," NASA TM 78687, July 1978 (N78-33480).

[7]Crawford, R. F. and Benton, M. D., "Strength of Initially Wavy Lattice Columns," *AIAA Journal*, Vol. 18, May 1980, pp. 581-584.

[8]Brebbia, C. A., *The Boundary Element Method for Engineers*, Pentech, London, 1980.

[9]Elyada, D., "Structural Analysis of Imperfect Three-Legged Truss Columns for Large Space Structures Applications," Thesis, California Institute of Technology, Pasadena, CA, Rept. SM 84-20, Dec. 1984.